International Journal of Nanomedicine

Dovepress
open access to scientific and medical research

Open Access Full Text Article

ORIGINAL RESEARCH

Combinatorial evaluation of in vivo distribution of polyanhydride particle-based platforms for vaccine delivery

This article was published in the following Dove Press journal:
International Journal of Nanomedicine
17 June 2013
Number of times this article has been viewed

Latrisha K Petersen[1]
Lucas Huntimer[2]
Katharine Walz[1]
Amanda Ramer-Tait[2]
Michael J Wannemuehler[2]
Balaji Narasimhan[1]

[1]Department of Chemical and Biological Engineering, Iowa State University, Ames, IA, USA; [2]Department of Veterinary Microbiology and Preventive Medicine, Iowa State University, Ames, IA, USA

Abstract: Several challenges are associated with current vaccine strategies, including repeated immunizations, poor patient compliance, and limited approved routes for delivery, which may hinder induction of protective immunity. Thus, there is a need for new vaccine adjuvants capable of multi-route administration and prolonged antigen release at the site of administration by providing a depot within tissue. In this work, we designed a combinatorial platform to investigate the in vivo distribution, depot effect, and localized persistence of polyanhydride nanoparticles as a function of nanoparticle chemistry and administration route. Our observations indicated that the route of administration differentially affected tissue residence times. All nanoparticles rapidly dispersed when delivered intranasally but provided a depot when administered parenterally. When amphiphilic and hydrophobic nanoparticles were administered intranasally, they persisted within lung tissue. These results provide insights into the chemistry- and route-dependent distribution and tissue-specific association of polyanhydride nanoparticle-based vaccine adjuvants.

Keywords: combinatorial, polyanhydride, nanoparticle, live animal imaging, distribution

Introduction

While vaccination is one of the most successful methods of disease prevention, many current strategies require frequent administrations to achieve protective immunity. Vaccines are primarily administered parenterally, often causing pain and leading to poor patient compliance.[1–4] Furthermore, the best way to achieve efficacy is by immunizing via mucosal surfaces, the same route that most pathogens use to infect the host.[5] In this regard, intranasal (IN) delivery has several advantages over parenteral routes for immunization against respiratory pathogens. This needle-free approach does not require highly trained medical personnel, results in better patient compliance, and is capable of enhancing both mucosal and systemic immune responses.[6] A drawback of IN administration is the relatively poor immune responses induced by soluble protein antigens that are used in nonadjuvanted vaccines.[2,6] Often, there is rapid epithelial adsorption and mucociliary clearance of these antigens,[6] which can result in short respiratory tract residence times and induction of weak immune responses.[7,8] Collectively, a need exists for versatile, biocompatible vaccine delivery platforms that can be administered via a variety of routes, thereby allowing them to reach different lymphoid tissues and provide sustained antigen release to enable more effective disease prevention.

Biodegradable polymers can provide sustained delivery of biological molecules, limiting the need for repeated administrations and improving patient compliance.[9–13]

Correspondence: Balaji Narasimhan
Department of Chemical and Biological Engineering, Iowa State University,
2035 Sweeney Hall, Ames,
IA 50011, USA
Tel +1 515 294 8019
Fax +1 515 294 9273
Email nbalaji@iastate.edu

This has beneficial implications for vaccine delivery, because it would promote continual antigen presentation and subsequently enhance the development of immunological memory.[14] Polyanhydrides are biodegradable, nontoxic, nonmutagenic materials capable of encapsulating and delivering biological molecules in vivo. These polymers can be formulated into nanoparticles for parenteral or IN administration.[12,13] Nanoparticles based upon copolymers of sebacic acid (SA), 1,6-bis-(*p*-carboxyphenoxy) hexane (CPH), and 1,8-bis-(*p*-carboxyphenoxy)-3,6-dioxaocatane (CPTEG) have been shown to exhibit tunable properties, including sustained antigen release kinetics, antigen stabilization, and immunomodulatory adjuvant behavior.[15–30] Recently in our laboratories, polyanhydride nanoparticles have been shown to induce less inflammation at administration sites than traditional adjuvants.[31] Additionally, histological evaluation revealed minimal toxicological effects and minimal adverse injection site reactions. Amphiphilic copolymers based on CPTEG and CPH have demonstrated the ability to enhance cell surface marker expression on dendritic cells similar to that induced by lipopolysaccharide (LPS) but without the toxic side effects caused by excessive cytokine production.[16,24,27,29] These properties of polyanhydride nanoparticles stimulate the immune system and enable the induction of immunological memory. Recently, long-term protection against a lethal challenge of *Yersinia pestis* was achieved with a single-dose IN vaccine regimen employing polyanhydride nanoparticles encapsulating the F1-V antigen.[13]

The goal of this work was to investigate the in vivo distribution of various polyanhydride nanoparticle formulations when administered to mice via different routes. These studies will provide insights that will enable the rational design of polyanhydride-based vaccine formulations that can optimally stimulate the immune system and induce long-term protective immunity. The studies described herein were performed using a combinatorial approach to simultaneously investigate the effect of nanoparticle chemistry and administration route on particle distribution in individual mice. Our observations indicate that route of administration differentially affects tissue residence times of the nanoparticles. All nanoparticles rapidly dispersed when delivered intranasally, but provided a depot when administered parenterally. In addition, intranasally administered amphiphilic and hydrophobic nanoparticles demonstrated persistence within lung tissue. These studies demonstrate that polyanhydride nanoparticles offer a versatile platform in which polymer chemistry and route of administration can be employed to rationally design vaccine regimens to combat current and emerging diseases.

Material and methods

Material

The chemicals utilized in the monomer synthesis include: 4-*p*-fluorobenzonitrile, purchased from Apollo Scientific (Cheshire, UK); 1-methyl-2-pyrrolidinone, 1,6-dibromohexane, tri-ethylene glycol, 4-hydroxybenzoic acid, 4-*p*- and 1,6-dibromohexane; these were purchased from Sigma Aldrich (St, Louis, MO, USA); and dimethyl formamide (DMF), toluene, sulfuric acid, acetonitrile, and potassium carbonate were obtained from Fisher Scientific (Fairlawn, NJ, USA). Chemicals for the polymer synthesis and nanoparticle fabrication, pentane, methylene chloride, acetic anhydride and chloroform, were all purchased from Fisher Scientific. Deuterated chemicals for nuclear magnetic resonance (NMR) analysis included chloroform and dimethyl sulfoxide (Cambridge Isotope Laboratories, Andover, MA, USA). Fluorescent dyes for in vivo imaging included: Texas Red®-X succinimidyl ester (TR) was purchased from Invitrogen (Carlsbad, CA, USA) and VivoTag 680 (VT680) and VivoTag 800 (VT800) were purchased from Perkin Elmer (Waltham, MA, USA). SKH1-E mice were obtained from Charles River (Wilmington, MA, USA) and housed under specific pathogen-free conditions. Animal procedures were conducted with the approval of the Iowa State University Institutional Animal Care and Use Committee.

Combinatorial polymer synthesis, nanoparticle fabrication, and characterization

SA monomer was purchased from Sigma Aldrich. CPH monomer and CPTEG were synthesized as described previously.[32] CPTEG:CPH and CPH:SA copolymers were combinatorially synthesized as described elsewhere.[27,28,33] Briefly, the monomers were dissolved in acetic anhydride (for CPTEG:CPH polymers) or chloroform (for CPH:SA polymers), robotically deposited into a multi-well substrate, and exposed to the necessary temperature (140°C for CPTEG:CPH or 180°C for CPH:SA) and vacuum (<0.3 torr) for 90 minutes. Following polymer library synthesis, nanoparticles were fabricated using a nonsolvent precipitation method. Briefly, the polymers were dissolved in methylene chloride, fluorescent dye was added to the dissolved polymer, the dye-polymer solution was dispersed by sonication at 40 Hz for 30 seconds, the solution poured into a nonsolvent (pentane), and the dye-loaded nanoparticle chemistries (~100% loading efficiency)

recovered by vacuum filtration. They were stored under dry conditions at −20°C until use in vivo. The polymers were characterized by ^{1}H NMR spectroscopy and gel permeation chromatography and the nanoparticles were imaged using scanning electron microscopy. The chemical structures of the monomers and representative images of the nanoparticles are shown in Figure S1.

Nanoparticle administration in vivo and image capture of mice and organs

Nanoparticles were suspended in sterile saline and sonicated at 15 Hz for 30 seconds to disperse the particles. Immunocompetent, hairless SKH-1 mice were chosen for these studies to reduce the autofluorescence of mouse fur and, thus, increase the resolution of the dye incorporated into the nanoparticles. The mice were anesthetized with isoflurane and administered 50 μL of the desired treatment (dye-loaded nanoparticles, dye only, or saline). In this study, three routes of administration were evaluated. The nanoparticles were injected subcutaneously (SC; at the nape of the neck) or intramuscularly (IM; thigh muscle) using a hypodermic needle and syringe; the intranasal (IN; via the nostrils) administrations were accomplished using a pipettor fitted with a pipet tip. The nanoparticle chemistries studied were 50:50 CPTEG:CPH, 50:50 CPH:SA, 20:80 CPTEG:CPH, and 20:80 CPH:SA. In the route-dependent study, 50:50 CPTEG:CPH or 50:50 CPH:SA nanoparticles were used. The particles administered SC were loaded with TR, those administered IN were loaded with VT800, and those administered IM were loaded with VT680. For the chemistry-dependent IN study, 50:50 CPTEG:CPH and 50:50 CPH:SA were loaded with VT680 and 20:80 CPTEG:CPH and 20:80 CPH:SA with VT800. Approximately 170 μg of dye-loaded nanoparticles were administered per route in the route dependent studies or per chemistry in the chemistry dependent studies. Control groups were included for each combinatorial study, which consisted of mice that only received one treatment. Additionally, dye only and saline were administered for each route to serve as controls for the live animal imaging. X-ray and fluorescent images of both the ventral and dorsal sides of each mouse were obtained at 3 hours, 6 hours, 12 hours, 24 hours, 3 days, 7 days, and 14 days using the In vivo Multispectral FX Pro imaging system (Carestream, Rochester, NY, USA). TR, VT680, and VT800 have excitation wavelengths of 540 nm, 670 nm, and 760 nm and emission wavelengths of 600 nm, 750 nm, and 830 nm, respectively. Images of the animals were obtained for anatomical localization of a fluorescent target. The 30 second X-ray exposures were captured using the X-ray device contained within the Multispectral FX Pro imaging System (kVp – 10 to 35 and 0.15 mA). On day 14, the mice were imaged and euthanized. Ex vivo tissue analysis of the liver, spleen, kidneys, lungs, and administration sites was performed to determine nanoparticle presence. The tissues were excised, washed with PBS, and imaged.

Image analysis

Sixteen bit mouse and organ tiff images were analyzed with Image J (NIH, Bethesda, MD, USA). Images were inverted and background was subtracted based upon a rolling ball radius of 50, 150, and 150 pixels from each image obtained using the excitation and emission combinations of 540 nm and 600 nm, 670 nm and 750 nm, and 760 nm and 830 nm, respectively. Images were stacked and regions of interest (ROIs) were created around each site of administration and around each organ (Figure 2F). Mean fluorescence intensity (MFI) was determined for each ROI of all the images. Image overlays were created by stacking the images, creating a color composite, and adjusting each channel to the desired color, brightness, and contrast. Macros were created and utilized to consistently analyze all images in determining ROI MFIs and in creating image overlays.

Data and statistical analysis

The MFI data were normalized to the saline group. JMP software (SAS Institute, Cary, NC, USA) was used to make comparisons between treatments and the negative (saline) control using the Student's *t*-test and comparisons between different treatments (route or chemistry) were performed using a model analysis of variance (ANOVA) with Tukey's HSD.

Results

Polymer and nanoparticle characterization

Proton NMR and gel permeation chromatography were used to determine the molecular weight and NMR was used to determine chemical structure of the combinatorially synthesized polyanhydrides. The polymers were found to have a molecular weight range (10,000 to 18,000 Da) that was in agreement with previously published work.[19–21,32] Previous work has demonstrated that molecular weights in this range have no effect on nanoparticle synthesis and result in similar particle sizes.[19–21,32] The thermal properties, hydrophobicities, and degradation rates of these polymers are shown in Table 1. Scanning electron microscopy images of the dye-loaded nanoparticles revealed average particle sizes of ~200 nm and uniform surface morphology across

Table 1 Polyanhydride thermal properties and contact angles[22,32,36,37,47]

Chemistry	T_g (°C)	Approximate % degradation after 30 days	Contact angle (°)
50:50 CPTEG:CPH	8	80%	45
20:80 CPTEG:CPH	18	40%	45
50:50 CPH:SA	6.1–11.5	70%	50
20:80 CPH:SA	50.0	80%	50

Abbreviations: CPH, 1,6-bis-(*p*-carboxyphenoxy) hexane; CPTEG, 1,8-bis-(*p*-carboxyphenoxy)-3,6-dioxaocatane; SA, sebacic acid.

chemistries, consistent with previous work, and representative images are shown in Figure S1D.[13,24,34] The chemical and structural characterization of the dye-loaded nanoparticles was also consistent across chemistries and batches and in agreement with previous work.[34]

Nanoparticle biodistribution and persistence is influenced by administration route

In these studies, amphiphilic 50:50 CPTEG:CPH or hydrophobic 50:50 CPH:SA nanoparticles were administered via three different routes: SC, IM, and IN. Nanoparticles administered by the different routes were each labeled with a different fluorescent dye: either TR (SC), VT680 (IM), or VT800 (IN). Due to the low molecular weight of the fluorescent dyes encapsulated into the nanoparticles, rapid dye clearance is expected upon release from the nanoparticles; this indicates that any fluorescence detected within a given ROI corresponds to encapsulated dye and not to that of released dye. Figure 1 depicts representative time course images of mice administered 50:50 CPTEG:CPH (M1) or 50:50 CPH:SA nanoparticles (M2) via the different routes. The IN nanoparticles rapidly dispersed into the respiratory tract and remained detectable in the nasal passages for approximately 24 hours, whereas the SC or IM nanoparticles persisted at the site of administration for at least 14 days (Figure 1). The time course images for each nanoparticle formulation administered individually are shown in Figure S2A.

A chronological comparison of the distribution and persistence patterns obtained after administration of 50:50 CPTEG:CPH or 50:50 CPH:SA nanoparticles is shown in Figure 2A and B, respectively. To assess the distribution of the intranasally administered nanoparticles throughout the mouse, ROI analyses of the head, neck, chest, and abdomen were performed after IN administration of 50:50 CPTEG:CPH or 50:50 CPH:SA nanoparticles (Figure 2C and D, respectively). In contrast to the dissemination of IN nanoparticles, the IM and SC administered nanoparticles resided at the site of administration. The hydrophobic 50:50 CPH:SA nanoparticles administered intramuscularly persisted the longest at the administration site as compared to their persistence when administered at the SC or IN sites (Figure 2). In contrast, the subcutaneously delivered amphiphilic 50:50 CPTEG:CPH nanoparticles persisted longer at the site of administration when compared to similarly administered hydrophobic 50:50 CPH:SA particles, as indicated by higher MFI values at all time points. Both nanoparticle chemistries were found to behave similarly when administered intranasally, rapidly disseminating throughout the body and becoming undetectable

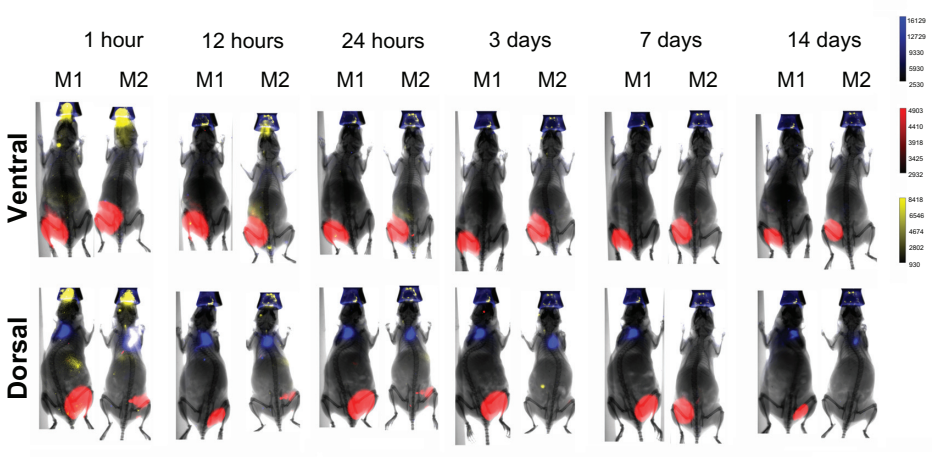

Figure 1 Representative dorsal and ventral images of mice showing differential persistence of nanoparticles that were administered via three different routes.
Notes: IM particles were detected at >14 days, SC particles were detectable for ~14 days and IN particles were not detectable beyond one day. M1 = mouse administered 50:50 CPTEG:CPH nanoparticles and M2 = mouse administered 50:50 CPH:SA nanoparticles. Blue indicates TR-loaded particles administered SC, red indicates VT680-loaded particles administered IM, and yellow indicates VT800-loaded particles administered IN. Five mice were imaged per group and images from one representative mouse are shown.
Abbreviations: IM, intramuscular; IN, intranasal; SC, subcutaneous.

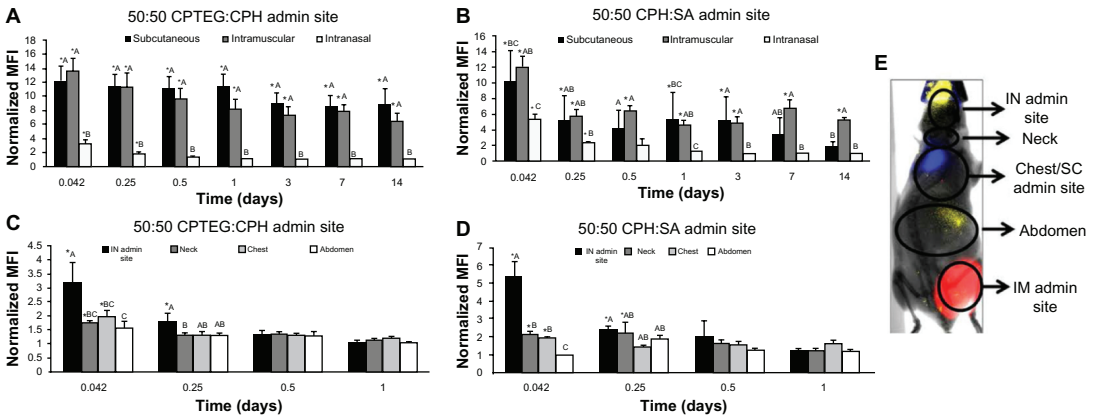

Figure 2 Nanoparticles administered via three different routes persisted at the administration site longest when administered IM, whereas IN particles rapidly disseminated throughout the body.

Notes: Analysis of nanoparticle fluorescence from Figure 1 revealed that 50:50 CPTEG:CPH (**A**) particles persisted at SC and IM administration sites longer than did 50:50 CPH:SA (**B**) particles 50:50 CPTEG:CPH (**C**) and 50:50 CPH:SA (**D**) nanoparticle biodistribution when administered IN suggested that both chemistries rapidly dispersed throughout the mouse within the first 24 hours. MFI values of all treatment groups were normalized to the saline control (saline normalized MFI = 1). Dorsal mouse image depicting the ROIs for each of the regions analyzed for fluorescence (**E**) Letters indicate statistical significance between each treatment group and asterisks indicate statistical significance (P-value < 0.05) from the saline control, n = 5 for 50:50 CPTEG:CPH and n = 3 for 50:50 CPH:SA.

Abbreviations: Admin, administration; CPH, 1,6-bis-(*p*-carboxyphenoxy) hexane; CPTEG, 1,8-bis-(*p*-carboxyphenoxy)-3,6-dioxaocatane; IN, intranasal; IM, intramuscular; MFI, mean fluorescence intensity; ROIs, regions of interest; SA, sebacic acid; SC, subcutaneous.

after 24 hours (Figure 2C and D). Importantly, there was no evidence that the delivery of nanoparticles by more than one route interfered with particle distribution emanating from the other sites (Figure S2). Specifically, the pattern and timing of nanoparticle distribution in mice administered nanoparticles at a single site were similar to those observed in mice administered nanoparticles at all three sites (Figure S2A and B).

Despite undetectable fluorescence in mice after 24 hours, examination of excised lungs indicated that nanoparticles were still present after 14 days (Figure 3 and Figure S3). It is important to note that the lack of fluorescence in the intact mouse images upon IN delivery of the nanoparticles (Figures 1 and 2) is likely due to the fluorescent signal dropping below the limit of detection in deep tissue and not because of the complete erosion of the nanoparticles.[35] Additionally, the ROI analysis indicated that while similar levels of fluorescence were observed in the whole mouse images at the SC and IM administration sites (Figure 2), actual fluorescence at the administration site was greatest for the IM nanoparticles (Figure 3). This is likely influenced by both the erosion kinetics of the particles when exposed to different tissue characteristics associated with the various administration sites as well as possible differences in immune

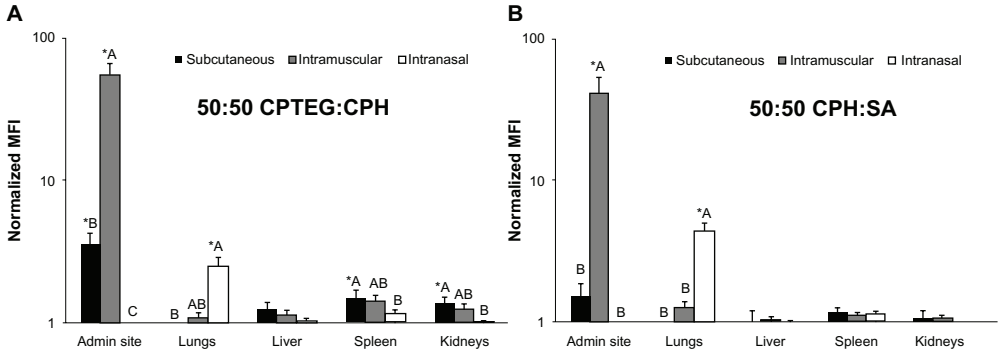

Figure 3 Nanoparticles were retained at the IM administration site longer than at the SC and IN sites of administration, as determined by ex vivo tissue ROI analysis 14 days after administration.

Notes: Nanoparticles administered IN were associated with the lungs and detectable for at least 14 days for both 50:50 CPTEG:CPH (**A**) and 50:50 CPH:SA (**B**) nanoparticles. Low level (50:50 CPTEG:CPH) to no (50:50 CPH:SA) nanoparticle fluorescence was observed in the liver, spleen, or kidneys. MFI values for all treatment groups were normalized to the saline control as described in the material and methods section (saline normalized MFI = 1). Letters indicate statistical significance between each treatment group and asterisks indicate statistical significance (P-value < 0.05) from the saline control, n = 5 for 50:50 CPTEG:CPH and n = 3 for 50:50 CPH:SA. Y-axis is presented in log scale.

Abbreviations: Admin, administration; CPH, 1,6-bis-(*p*-carboxyphenoxy) hexane; CPTEG, 1,8-bis-(*p*-carboxyphenoxy)-3,6-dioxaocatane; IN, intranasal; IM, intramuscular; MFI, mean fluorescence intensity; SA, sebacic acid; SC, subcutaneous.

cell trafficking at these sites. These findings indicate that the IM nanoparticles provided for the longest residence time as compared to the SC or IN administered nanoparticles. However, the SC and IN nanoparticles disseminated more rapidly than the IM nanoparticles.

Nanoparticle chemistry dictates lung association and persistence

In these studies, the effect of nanoparticle chemistry on persistence within and association with lung tissue upon IN administration was investigated. Figure 4 depicts representative time course images of mice that were intranasally administered both 20:80 and 50:50 CPTEG:CPH nanoparticles (M1) or both 20:80 and 50:50 CPH:SA nanoparticles (M2) simultaneously. It is clear that both CPTEG:CPH and CPH:SA nanoparticles disseminated rapidly throughout the body, consistent with the data shown in Figure 1. Further analysis of these images revealed that most nanoparticles were undetectable after 24 hours. Figure S4 shows each fluorescent image captured independently and provides visualization of the in vivo distribution of each individual nanoparticle formulation. The ROI analysis of the data in Figure 4 is summarized in Figure 5. The 20:80 CPH:SA nanoparticles distributed the most rapidly throughout the body and were detectable at significantly greater levels than the other nanoparticle chemistries in the abdomen after 3 hours. After IN administration, all other nanoparticle chemistries appeared to distribute similarly throughout the body, disseminating from the head to abdomen within the first 24 hours. Mice administered each individual nanoparticle formulation exhibited similar distribution patterns to those of mice administered multiple formulations (Figure S4B).

Despite the inability to detect fluorescence in vivo after 24 hours, ex vivo analysis of the organs 14 days after IN administration revealed that all nanoparticle formulations (independent of chemistry) were detectable in the lung tissue (Figure 6 and Figure S5). This observation indicates that all nanoparticle formulations persisted in the lungs for at least 14 days.

Discussion

Polyanhydride particles present compelling advantages as vaccine adjuvants in comparison to traditional adjuvants such as Alum and monophosphoryl lipid A (MPLA) because of their ability to provide robust immune responses in a single dose, their versatility in terms of delivery routes, their ability to induce long-lived, high titer and highly avid antibody, their activation of antigen presenting cells, and their polymer chemistry-dependent antigen-specific activation of $CD4^+$ and $CD8^+$ T cells.[13,16,24,27] To further understand their distribution and tissue association in vivo, we utilized a combinatorial approach to simultaneously investigate the effect of administration route and nanoparticle chemistry. This approach facilitated the simultaneous evaluation of multiple parameters (ie, particle chemistry and administration route) per mouse,

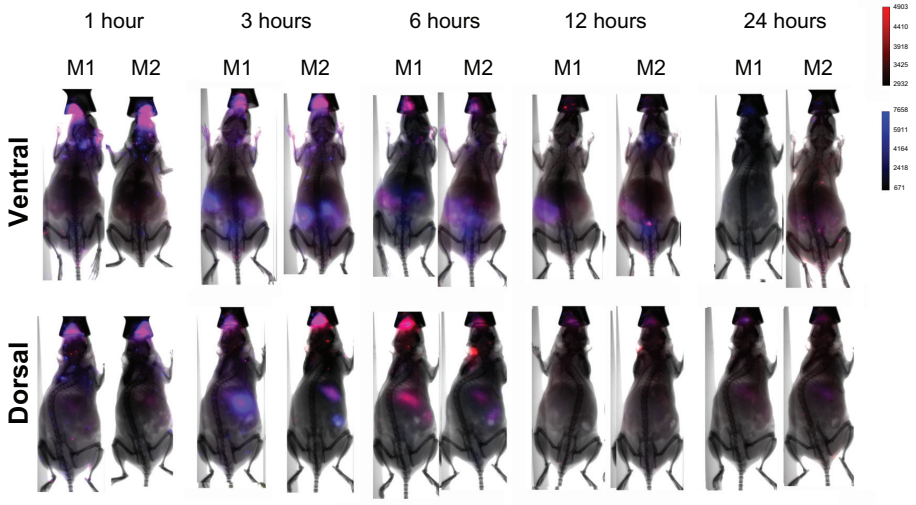

Figure 4 Representative mouse images depicting the detection of two nanoparticle formulations, 50:50 and 20:80 CPH:SA or 50:50 and 20:80 CPTEG:CPH, that were simultaneously administered IN.

Notes: The results demonstrate a rapid dispersion of particles of both chemistries throughout the body after administration. The data show that CPTEG:CPH nanoparticles tended to localize in different tissue regions than CPH:SA nanoparticles. M1 = mouse administered VT680-loaded 50:50 CPTEG:CPH nanoparticles IN (red) and VT800-loaded 20:80 CPTEG:CPH nanoparticles (blue) and M2 = mouse administered VT680-loaded 50:50 CPH:SA nanoparticles IN (red) and 20:80 CPH:SA VT800-loaded nanoparticles IN (blue). Three mice were imaged per group and images from one representative mouse are shown.

Abbreviations: CPH, 1,6-bis-(*p*-carboxyphenoxy) hexane; CPTEG, 1,8-bis-(*p*-carboxyphenoxy)-3,6-dioxaocatane; IN, intranasal; SA, sebacic acid.

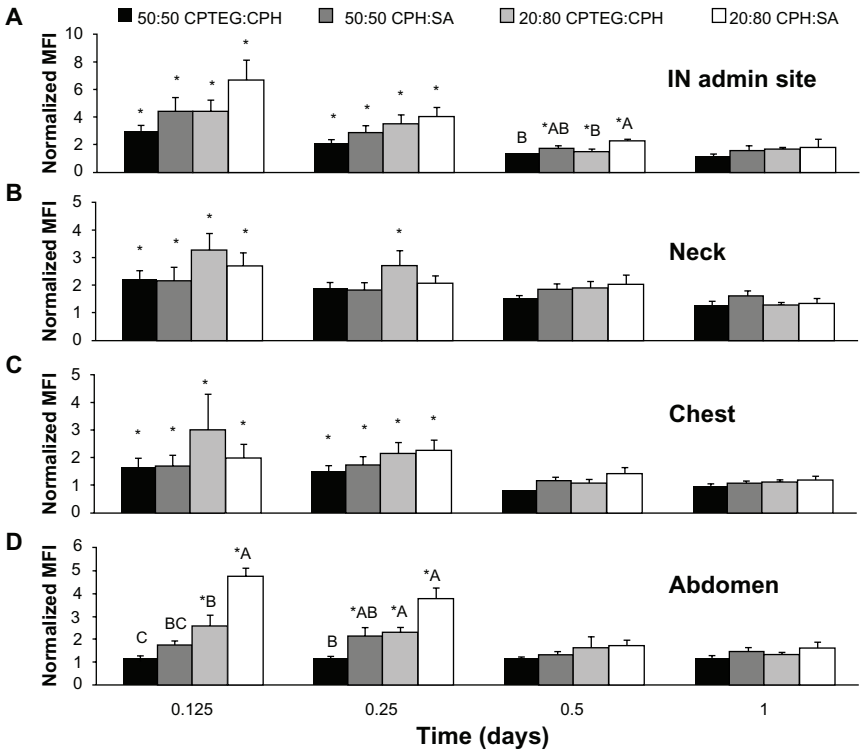

Figure 5 Polyanhydride chemistry played an important role in nanoparticle distribution throughout the body.

Notes: Analysis of nanoparticle fluorescence from Figure 4 for the following regions: (**A**) nasal passage, (**B**) neck, (**C**) chest, and (**D**) abdomen. The 20:80 CPH:SA nanoparticles show significantly greater fluorescence in the lower abdomen at 3 hours (0.125 days). MFI values for all treatment groups were normalized to the saline control (saline normalized MFI = 1). A dorsal mouse image depicting the ROIs for each of the mouse regions can be seen in Figure 2E. Letters indicate statistical significance between each treatment group and asterisks indicate statistical significance (P-value < 0.05) from the saline control, n = 3 for all groups.

Abbreviations: Admin, administration; CPH, 1,6-bis-(*p*-carboxyphenoxy) hexane; CPTEG, 1,8-bis-(*p*-carboxyphenoxy)-3,6-dioxaocatane; IN, intranasal, MFI, mean fluorescence intensity; ROI, region of interest; SA, sebacic acid.

thereby reducing the number of experimental subjects, time, and cost. These studies revealed that polyanhydride nanoparticles persisted at the parenteral administration sites (IM and SC) or in lung tissue (IN). This approach also enabled the characterization of the distribution of a particular nanoparticle formulation away from a given site when particles were administered at other sites. The findings provide a framework for a multi-route vaccination strategy enabling simultaneous immunization against multiple pathogens.

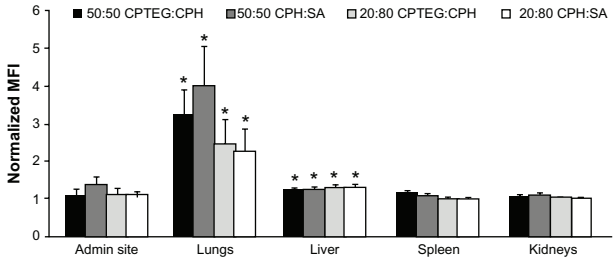

Figure 6 Evaluation of excised organs for the presence of fluorescently labeled nanoparticles 14 days after intranasal administration.

Notes: Even though no longer visible in the whole mouse images, all nanoparticle chemistries administered IN were detected in the excised lungs for at least 14 days, as determined by ex vivo tissue analysis. At day 14, no nanoparticle fluorescence was observed in the liver, spleen, or kidneys. MFI values of all treatment groups were normalized to the saline control (saline normalized MFI = 1). Asterisks indicate statistical significance (P-value <0.05) from the saline control, n = 3 for all groups.

Abbreviations: CPH, 1,6-bis-(*p*-carboxyphenoxy) hexane; CPTEG, 1,8-bis-(*p*-carboxyphenoxy)-3,6-dioxaocatane; MFI, mean fluorescence intensity; SA, sebacic acid.

Our work demonstrated that polyanhydride nanoparticles persist at the site of administration for at least 2 weeks upon SC and IM delivery or within the lungs upon IN delivery (Figures 3 and 6). This observation suggests that polyanhydride nanoparticles will provide a sustained release of encapsulated antigen for that period of time. Further studies indicated that nanoparticles are still present at the site of injection after 2 months (SC) and 3 months (IM) (Figures 1 and 2 and data not shown). Upon examination of excised tissue samples, the presence of fluorescent nanoparticles was significantly greater for the IM particles than the SC or IN particles (Figure 3). The SC nanoparticles would have access to the lymphatics and immune cells to facilitate their dispersion. In addition to dispersing to the lungs, a portion of the IN nanoparticles would likely be swallowed and then taken up from the gastrointestinal tract (eg, Peyer's patches). Unlike SC or IM routes of administration, these two paths of particle fate would contribute

to the pattern of particle distribution observed following IN administration.

Together, these data indicate that route of nanoparticle administration differentially affected their residence times at the site of administration. This finding, in combination with the ability to tailor the erosion kinetics of polyanhydride nanoparticles, suggests that in vivo antigen delivery could be designed to occur over a specific time frame (eg, days to months).[32,36,37] This finding has important implications for the design of single dose vaccines. Kipper et al demonstrated that a single dose of polyanhydride particles administered parenterally to mice was sufficient to stimulate high-titer antibody production and antigen-specific lymphocyte proliferation twelve weeks after administration.[12] This observation was extended by Huntimer et al who showed that parenteral administration of particles provided sustained release of ovalbumin and allowed for at least a 16-fold dose reduction in the dose of antigen required for induction of an equivalent antibody production induced by soluble protein alone.[38] Finally, Ulery et al demonstrated that a single IN dose of amphiphilic nanoparticles, together with soluble antigen, provided long-term protective immunity against lethal challenge with *Y. pestis*.[13] In all these studies, it was hypothesized that the slow erosion of the particles enabled persistent antigen presentation by antigen presenting cells (APCs), thereby promoting affinity maturation of B cells and the development of a high titer, high avidity antibody response. The persistence of the nanoparticles observed in the present work, influenced by particle chemistry and administration route, demonstrates a beneficial characteristic of these nanoparticles compared to traditional adjuvants such as Alum or MPLA for the development of single dose vaccines.

While IM administration is used for many current vaccines, immunization via alternate routes, including mucosal surfaces, could significantly enhance vaccine efficacy. IN vaccination is an advantageous delivery method to immunize against respiratory pathogens, such as seasonal influenza virus, group A *Streptococcus*, or aerosolized *Bacillus anthracis*. However, the relatively poor immune response induced by nonadjuvanted antigens and high probability of mucociliary clearance often render IN vaccination ineffective.[6,39,40] Thus, parenteral immunization with adjuvanted subunit vaccines has been primarily used against respiratory pathogens. One limitation of parenteral vaccination is the induction of predominantly serum IgG against the vaccine antigen with little production of secretory IgA, consequently limiting immune protection at mucosal surfaces.[6] The polyanhydride nanoparticles discussed in this work can be effectively administered intranasally to enhance the induction of a mucosal immune response. Furthermore, they are capable of sustained antigen release and the activation of APCs, which contributes to the induction of high titer and high avidity antibody responses.[16,18–20,22,24,25,27–29] In the current work, only the IN nanoparticles dispersed rapidly throughout the body (Figures 1 and 2) and demonstrated prolonged residence in lung tissue (Figures 3 and 6). This enhanced persistence of nanoparticles in the lungs may provide a sufficient depot for antigen release, immune stimulation, and robust antibody production as observed previously.[13,14,41]

The present work has also demonstrated that polymer chemistry plays an integral role in tissue residence time and distribution of nanoparticles delivered intranasally (Figures 4–6). Adjuvant chemistry dictates properties such as hydrophobicity, glass transition temperature (T_g), degradation kinetics, exposed end groups, etc, that are hypothesized to influence biodistribution and persistence.[27,29] In this work, the 20:80 CPH:SA nanoparticles dispersed throughout the body most rapidly (Figures 4 and 5). This observation may be attributed to a combination of low hydrophobicity and high T_g (Table 1). These properties may enable the 20:80 CPH:SA nanoparticles to disseminate more rapidly throughout the body without preferentially associating with the lungs. In contrast, the low T_g nanoparticles (ie, 50:50 CPTEG:CPH and 50:50 CPH:SA) are more malleable and can change shape as dictated by their environment,[27,29] which may explain their strong association with lung tissue (Figure 6). Indeed, structural and thermal similarities have been identified among these nanoparticles, pathogens, and common surface molecules of pathogens (eg, LPS)[27,29,42,43] that may explain why the lung tissue association of nanoparticles effectively induces a robust antibody response. Pathogens persist at mucosal surfaces resulting in chronic colonization of the respiratory tract. Therefore, intervention strategies employing nanoparticles that mimic the persistence of respiratory pathogens may prove to be more efficacious than traditional vaccinations.

In addition to polymer T_g, hydrophobicity is known to play an important role in mucosal transport, with the least hydrophobic particles having the highest rate of translocation.[44] Szentkuti reported that hydrophobic latex nanoparticles (<415 nm) rapidly penetrated the mucus layer and attached to the apical membranes of epithelial cells, indicating that they are cell-tropic rather than mucoadhesive.[45] Other studies have shown that the least hydrophobic polyanhydride nanoparticles (SA- and CPTEG-rich) are the most readily internalized by APCs.[26,27]

However, to enable sufficient internalization by immune cells (eg, alveolar macrophages) in the lung, the nanoparticle chemistry must be capable of lung tissue association. Given this consideration, the amphiphilic 50:50 CPTEG:CPH formulation, with its ability to enhance both persistence and uptake, may be an "optimal" candidate for an IN nanoparticle delivery platform. Other structural properties, including the presence of hydroxyl end groups, have been shown to influence bioadhesive interactions to mucosal surfaces caused by increased hydrogen bonding.[46] Degradation of polyanhydride nanoparticles results in the formation of hydroxyl end groups that, as suggested, may promote hydrogen bonding and result in strong interactions with the lung tissue. Thus, the more rapidly degrading chemistries (ie, 50:50 CPTEG:CPH) with low T_gs may provide the best option for treatment or vaccination via the respiratory tract. The 50:50 CPTEG:CPH nanoparticles displayed longer persistence within the lungs than did the other formulations (Figures 4 and 6), making the particles more accessible to APCs for uptake and subsequent APC activation and migration to draining lymph nodes.[27,29] Following IN administration, polyanhydride nanoparticles demonstrated longer persistence within the nasal passages than other polymer-based systems, such as N,N,N-trimethyl chitosan, indicating that polyanhydride nanoparticles may be more effective for immunization against respiratory pathogens.[39]

Conclusion

The combinatorial in vivo studies described herein demonstrated a chemistry- and route-dependent in vivo distribution and persistence of polyanhydride nanoparticles. Amphiphilic 50:50 CPTEG:CPH nanoparticles demonstrated the longest residence time at parenteral administration sites and would be expected to provide a long-term antigen depot. Additionally, the low T_g 50:50 CPTEG:CPH and 50:50 CPH:SA nanoparticles demonstrated longer persistence in lung tissue following IN administration, emphasizing their value as a vaccine delivery system against respiratory pathogens. Furthermore, as indicated by the combinatorial approach, there was no interference of nanoparticle distribution when particles were simultaneously administered by multiple routes. This finding indicates that a strategy for multiple site immunization against one or more pathogens could be developed using this platform. The insights gained from these studies will facilitate the rational design of a nanoparticle-based platform for localized delivery of vaccines to prevent current and emerging respiratory infectious diseases.

Acknowledgments

The authors would like to acknowledge financial support from the ONR-MURI Award (NN00014-06-1-1176), the ONR-DURIP Award (N00014-09-1-0851), and the US Army Medical Research and Materiel Command (Grant No W81XWH-09-1-0386). This material is based upon work supported by the National Science Foundation under Grant No EEC 0851519 to B.N.

Disclosure

The authors report no conflicts of interest in this work.

References

1. Tournier JN, Ulrich RG, Quesnel-Hellmann A, Mohamadzadeh M, Stiles BG. Anthrax, toxins and vaccines: a 125-year journey targeting Bacillus anthracis. *Expert Rev Anti Infect Ther*. 2009;7(2):219–236.
2. Mitragotri S. Immunization without needles. *Nat Rev Immunol*. 2005; 5(12):905–916.
3. Aguado MT, Lambert PH. Controlled-release vaccines – biodegradable polylactide/polyglycolide (PL/PG) microspheres as antigen vehicles. *Immunobiology*. 1992;184(2–3):113–125.
4. Watson-Creed G, Saunders A, Scott J, Lowe L, Pettipas J, Hatchette TF. Two successive outbreaks of mumps in Nova Scotia among vaccinated adolescents and young adults. *CMAJ*. 2006;175(5):483–488.
5. Wilson-Welder JH, Torres MP, Kipper MJ, Mallapragada SK, Wannemuehler MJ, Narasimhan B. Vaccine adjuvants: current challenges and future approaches. *J Pharm Sci*. 2009;98(4):1278–1316.
6. Sanders MT, Deliyannis G, Pearse MJ, McNamara MK, Brown LE. Single dose intranasal immunization with ISCOMATRIX vaccines to elicit antibody-mediated clearance of influenza virus requires delivery to the lower respiratory tract. *Vaccine*. 2009;27(18):2475–2482.
7. Mikszta JA, Sullivan VJ, Dean C, et al. Protective immunization against inhalational anthrax: a comparison of minimally invasive delivery platforms. *J Infect Dis*. 2005;191(2):278–288.
8. Flick-Smith HC, Eyles JE, Hebdon R, et al. Mucosal or parenteral administration of microsphere-associated Bacillus anthracis protective antigen protects against anthrax infection in mice. *Infect Immun*. 2002;70(4):2022–2028.
9. Jain JP, Modi S, Domb AJ, Kumar N. Role of polyanhydrides as localized drug carriers. *J Control Release*. 2005;103(3):541–563.
10. Katti DS, Lakshmi S, Langer R, Laurencin CT. Toxicity, biodegradation and elimination of polyanhydrides. *Adv Drug Deliv Rev*. 2002; 54(7):933–961.
11. Torres MP, Determan AS, Mallapragada SK, Narasimhan B. Polyanhydrides. In: Lee S, Dekker M, editors. *Encyclopedia of Chemical Processing*. New York: Taylor and Francis; 2006:2247–2257.
12. Kipper MJ, Wilson JH, Wannemuehler MJ, Narasimhan B. Single dose vaccine based on biodegradable polyanhydride microspheres can modulate immune response mechanism. *J Biomed Mater Res A*. 2006;76A(4):798–810.
13. Ulery BD, Kumar D, Ramer-Tait A, Metzger DW, Wannemuehler MJ, Narasimhan B. Design of a protective single-dose intranasal nanoparticle-based vaccine platform for respiratory infectious diseases. *PLoS ONE*. 2011;6:e17642.
14. Zinkernagel RM. Localization dose and time of antigens determine immune reactivity. *Semin Immunol*. 2000;12(3):163–171.
15. Carrillo-Conde B, Song EH, Chavez-Santoscoy A, et al. Mannose-functionalized "pathogen-like" polyanhydride nanoparticles target C-type lectin receptors on dendritic cells. *Mol Pharm*. 2011;8(5):1877–1886.
16. Torres MP, Wilson-Welder J, Lopac SK, et al. Polyanhydride microparticles enhance dendritic cell antigen presentation and activation. *Acta Biomater*. 2011;7:2857–2864.

17. Carrillo-Conde B, Garza A, Anderegg J, Narasimhan B. Protein adsorption on biodegradable polyanhydride microparticles. *J Biomed Mater Res A*. 2010;95(1):40–48.
18. Carrillo-Conde B, Schiltz E, Yu J, et al. Encapsulation into amphiphilic polyanhydride microparticles stabilizes *Yersinia pestis* antigens. *Acta Biomater*. 2010;6(8):3110–3119.
19. Determan AS, Graham JR, Pfeiffer KA, Narasimhan B. The role of microsphere fabrication methods on the stability and release kinetics of ovalbumin encapsulated in polyanhydride microspheres. *J Microencaps*. 2006;23(8):832–843.
20. Determan AS, Trewyn BG, Lin VS, Nilsen-Hamilton M, Narasimhan B. Encapsulation, stabilization, and release of BSA-FITC from polyanhydride microspheres. *J Control Release*. 2004;100(1):97–109.
21. Determan AS, Wilson JH, Kipper MJ, Wannemuehler MJ, Narasimhan B. Protein stability in the presence of polymer degradation products: consequences for controlled release formulations. *Biomaterials*. 2006;27(17):3312–3320.
22. Lopac SK, Torres MP, Wilson-Welder JH, Wannemuehler MJ, Narasimhan B. Effect of polymer chemistry and fabrication method on protein release and stability from polyanhydride microspheres. *J Biomed Mater Res B Appl Biomater*. 2009;91(2):938–947.
23. Petersen LK, Determan AS, Westgate C, Bendickson L, Nilsen- Hamilton M, Narasimhan B. Lipocalin-2-loaded amphiphilic polyanhydride microparticles accelerate cell migration. *J Biomater Sci Polym Ed*. 2011;22:1237–1252.
24. Petersen LK, Xue L, Wannemuehler MJ, Rajan K, Narasimhan B. The simultaneous effect of polymer chemistry and device geometry on the in vitro activation of murine dendritic cells. *Biomaterials*. 2009;30(28):5131–5142.
25. Torres MP, Determan AS, Anderson GL, Mallapragada SK, Narasimhan B. Amphiphilic polyanhydrides for protein stabilization and release. *Biomaterials*. 2007;28(1):108–116.
26. Ulery BD, Phanse Y, Sinha A, Wannemuehler MJ, Narasimhan B, Bellaire BH. Polymer chemistry influences monocytic uptake of polyanhydride nanospheres. *Pharm Res*. 2009;26(3):683–690.
27. Petersen LK, Ramer-Tait A, Broderick S, et al. Activation of innate immune responses in a pathogen-mimicking manner by amphiphilic polyanhydride nanoparticle adjuvants. *Biomaterials*. 2011;32:6815–6822.
28. Petersen LK, Sackett CK, Narasimhan B. Novel, high throughput method to study in vitro protein release from polymer nanospheres. *J Comb Chem*. 12(1):51–56.
29. Ulery BD, Petersen LK, Phanse Y, et al. Rational design of pathogen-mimicking amphiphilic materials as nanoadjuvants. *Sci Rep*. 2011;1:198.
30. Petersen LK, Phanse Y, Ramer-Tait AE, Wannemuehler MJ, Narasimhan B. Amphiphilic polyanhydride nanoparticles stabilize *Bacillus anthracis* protective antigen. *Mol Pharm*. 9(4):874–882.
31. Huntimer L, Ramer-Tait AE, Petersen LK, et al. Evaluation of biocompatibility and administration site reactogenicity of polyanhydride-particle-based platform for vaccine delivery. *Adv Healthc Mater*. 2013;2(2):369–378.
32. Torres MP, Vogel BM, Narasimhan B, Mallapragada SK. Synthesis and characterization of novel polyanhydrides with tailored erosion mechanisms. *J Biomed Mater Res A*. 2006;76(1):102–110.
33. Adler AF, Petersen LK, Wilson JH, et al. High throughput cell-based screening of biodegradable polyanhydride libraries. *Comb Chem High Throughput Screen*. 2009;12(7):634–645.
34. Petersen LK, Sackett CK, Narasimhan B. High-throughput analysis of protein stability in polyanhydride nanoparticles. *Acta Biomater*. 2010;6(10):3873–3881.
35. Lyons SK. Advances in imaging mouse tumour models in vivo. *J Pathol*. 2005;205(2):194–205.
36. Shen E, Kipper MJ, Dziadul B, Lim MK, Narasimhan B. Mechanistic relationships between polymer microstructure and drug release kinetics in bioerodible polyanhydrides. *J Control Release*. 2002;82(1):115–125.
37. Shen E, Pizsczek R, Dziadul B, Narasimhan B. Microphase separation in bioerodible copolymers for drug delivery. *Biomaterials*. 2001;22(3):201–210.
38. Huntimer L, Wilson Welder JH, Ross K, et al. Single immunization with a suboptimal antigen dose encapsulated into polyanhydride microparticles promotes high titer and avid antibody responses. *J Biomed Mater Res B Appl Biomater*. 2013;101(1):91–98.
39. Hagenaars N, Mania M, de Jong P, et al. Role of trimethylated chitosan (TMC) in nasal residence time, local distribution and toxicity of an intranasal influenza vaccine. *J Control Release*. 2010;144(1):17–24.
40. Park HS, Francis KP, Yu J, Cleary PP. Membranous cells in nasal-associated lymphoid tissue: a portal of entry for the respiratory mucosal pathogen group A streptococcus. *J Immunol*. 2003;171(5):2532–2537.
41. Zinkernagel RM. *The Vaccine Book*, 1st ed. San Diego: Academic Press; 2003.
42. Ramos-Sanchez MC, Rodriguez-Torres A, Leal JA, Martin-Gil FJ, Martin-Gil J. Thermolytical techniques to characterize fungal polysaccharides and bacterial lipopolysaccharides. *Biotechnol Prog*. 1991;7(6):526–533.
43. Rodriguez-Torres A, Ramos-Sanchez MC, Orduna-Domingo A, Martin-Gil FJ, Martin-Gil J. Differential scanning calorimetry investigations on LPS and free lipids A of the bacterial cell wall. *Res Microbiol*. 1993;144(9):729–740.
44. Norris DA, Sinko PJ. Effect of size, surface charge, and hydrophobicity on the translocation of polystyrene microspheres through gastrointestinal mucin. *J Appl Polym Sci*. 1997;63(11):1481–1492.
45. Szentkuti L. Light microscopical observations on luminally administered dyes, dextrans, nanospheres and microspheres in the preepithelial mucus gel layer of the rat distal colon. *J Control Release*. 1997;46(3):233–242.
46. Agüeros M, Areses P, Campanero MA, et al. Bioadhesive properties and biodistribution of cyclodextrin-poly(anhydride) nanoparticles. *Eur J Pharm Sci*. 2009;37(3–4):231–240.
47. Mathiowitz E, Ron E, Mathiowitz G, Amato C, Langer R. Morphological characterization of bioerodible polymers 1. Crystallinity of polyanhydride copolymers. *Macromolecules*. 1990;23(13):3212–3218.

Supplementary figures

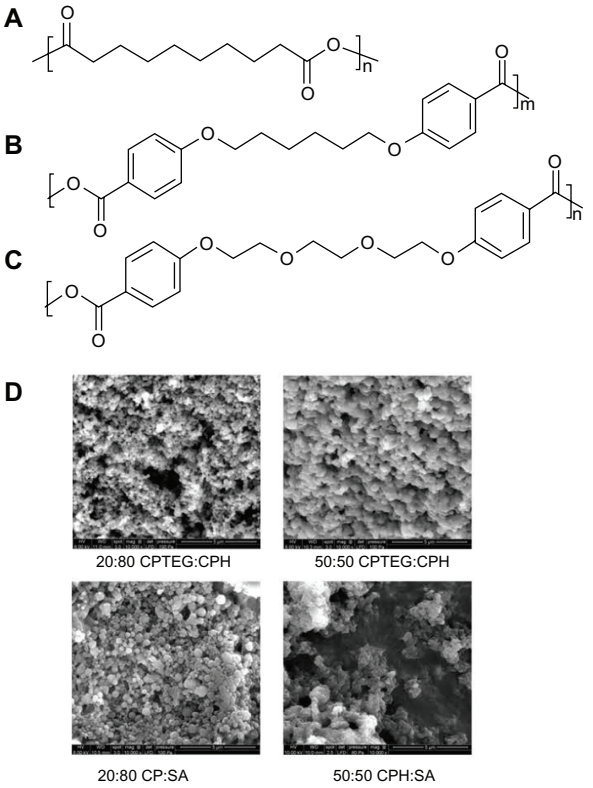

Figure S1 Chemical structures of SA (**A**) CPH (**B**) and CPTEG (**C**) monomers and representative SEM images (**D**) of all the nanoparticle formulations fabricated in this work.
Abbreviations: CPH, 1,6-bis-(*p*-carboxyphenoxy) hexane; CPTEG, 1,8-bis-(*p*-carboxyphenoxy)-3,6-dioxaocatane; SA, sebacic acid; SEM, scanning electron microscope.

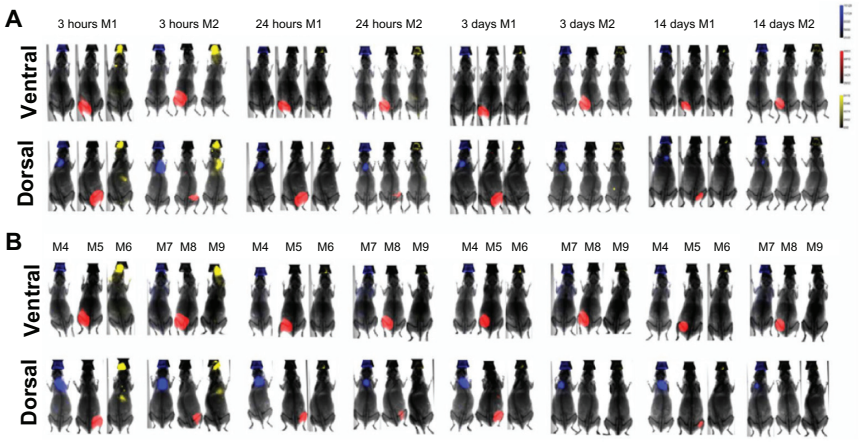

Figure S2 Administration of nanoparticles via three different routes simultaneously to the same mouse resulted in similar nanoparticle distribution patterns as compared to administration of nanoparticles via each route separately.
Notes: Representative mouse images from Figure 1 separated by filter channel (**A**) M1 = mouse administered 50:50 CPTEG:CPH nanoparticles and M2 = mouse administered 50:50 CPH:SA nanoparticles. Images of mice that received administration of nanoparticles via only one route (**B**) M4 = mouse administered 50:50 CPTEG:CPH SC, M5 = mouse administered 50:50 CPTEG:CPH IM, M6 = mouse administered 50:50 CPTEG:CPH IN, M7 = mouse administered 50:50 CPH:SA SC, M8 = mouse administered 50:50 CPH:SA IM, and M9 = mouse administered 50:50 CPH:SA IN. Blue indicates TR-loaded particles administered SC, red indicates VT680-loaded particles administered IM, and yellow indicates VT800-loaded particles administered IN.
Abbreviations: CPH, 1,6-bis-(*p*-carboxyphenoxy) hexane; CPTEG, 1,8-bis-(*p*-carboxyphenoxy)-3,6-dioxaocatane; IM, intramuscular; IN, intranasal; SA, sebacic acid; SC, subcutaneous.

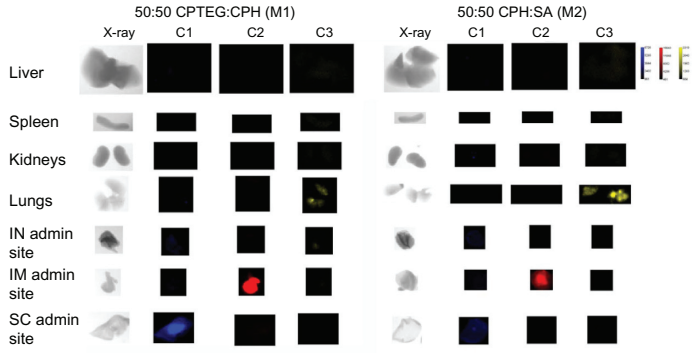

Figure S3 Representative 14 day organ images corresponding to Figure 3 separated by filter channel which indicate that IN administered 50:50 CPTEG:CPH and 50:50 CPH:SA nanoparticles (yellow) are detectable in the lung tissue while IM (red) and SC (blue) administered nanoparticles were primarily observed at the site of administration.

Notes: X-ray, C1-ex: 540 nm and em: 600 nm; C2-ex: 670 nm and em: 750 nm; C3-ex: 760 nm and em: 830 nm images were acquired. M1 = mouse administered 50:50 CPTEG:CPH nanoparticles and M2 = mouse administered 50:50 CPH:SA nanoparticles. Blue indicates TR-loaded particles administered SC, red indicates VT680-loaded particles administered IM, and yellow indicates VT800-loaded particles administered IN.

Abbreviations: Admin, administration; C, channel; CPH, 1,6-bis-(*p*-carboxyphenoxy) hexane; CPTEG, 1,8-bis-(*p*-carboxyphenoxy)-3,6-dioxaocatane; em, emission; ex, excitation; IM, intramuscular; IN, intranasal; SA, sebacic acid; SC, subcutaneous.

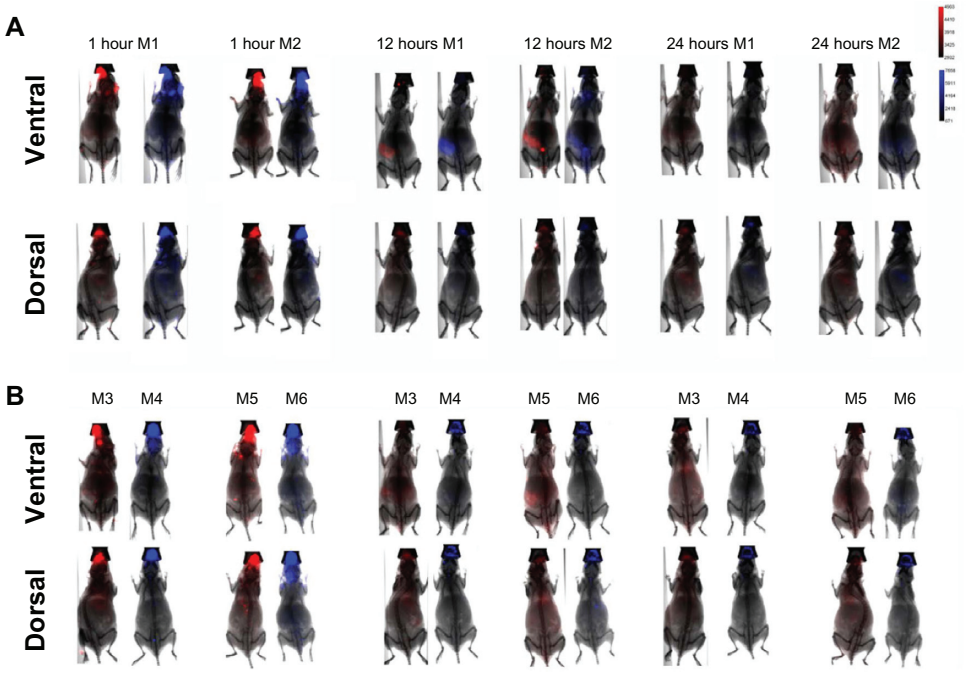

Figure S4 Each mouse administered nanoparticles of two different chemistries results in similar nanoparticle distribution compared to separate mice administered nanoparticles of each chemistry independently.

Notes: Representative mouse images from Figure 4 separated by filter channel which indicate that the nanoparticle of CPTEG:CPH chemistries may disperse differently than those of CPH:SA throughout the mouse body when administered IN (**A**) M1 = mouse administered VT680-loaded 50:50 CPTEG:CPH nanoparticles IN (red) and VT800-loaded 20:80 CPTEG:CPH nanoparticles (blue) and M2 = mouse administered VT680-loaded 50:50 CPH:SA nanoparticles IN (red) and 20:80 CPH:SA VT800-loaded nanoparticles IN (blue). Images of mice that received administration of nanoparticles with only one chemistry (**B**) M3 = mouse administered 50:50 CPTEG:CPH IN (red), M4 = mouse administered 20:80 CPTEG:CPH IN (blue), M5 = mouse administered 50:50 CPH:SA IN (red), and M6 = mouse administered 20:80 CPH:SA (blue).

Abbreviations: CPH, 1,6-bis-(*p*-carboxyphenoxy) hexane; CPTEG, 1,8-bis-(*p*-carboxyphenoxy)-3,6-dioxaocatane; IM, intramuscular; IN, intranasal; SA, sebacic acid; SC, subcutaneous.

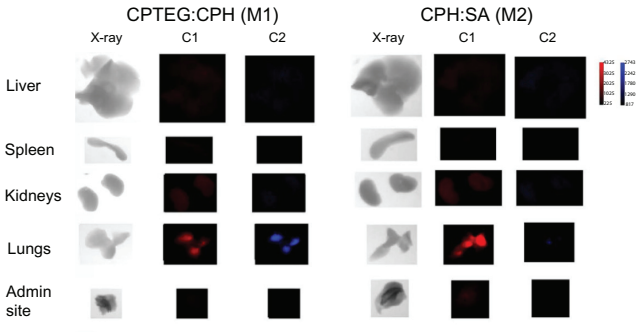

Figure S5 Representative 14 day organ images corresponding to Figure 6 separated by filter channels which indicate that IN administered nanoparticles are easily observed in the lung tissue even though they are no longer detectable in the whole mouse images.

Notes: X-ray, C1-ex: 540 nm and em: 750 nm, and C2-ex: 760 nm and em: 830 nm images were acquired. M1 = mouse administered VT680-loaded 50:50 CPTEG:CPH nanoparticles IN (red) and VT800-loaded 20:80 CPTEG:CPH nanoparticles (blue) and M2 = mouse administered VT680-loaded 50:50 CPH:SA nanoparticles IN (red) and 20:80 CPH:SA VT800-loaded nanoparticles IN (blue).

Abbreviations: Admin, administration; C, channel; CPH, 1,6-bis-(*p*-carboxyphenoxy) hexane; CPTEG, 1,8-bis-(*p*-carboxyphenoxy)-3,6-dioxaocatane; em, emission; ex, excitation; IM, intramuscular; IN, intranasal; SA, sebacic acid; SC, subcutaneous.